International Journal on Emerging Technologies 10(2): 78-93(2019)

ISSN No. (Print) : 0975-8364
ISSN No. (Online) : 2249-3255

A Convective Heat Flow in a Rectangular Cavity with Effect of Non-Isothermal Wall

K. Gayathri Devi[1] and K. Vijay Babu[2]

[1]Assistant Professor, S.R.E. College, Nandyal, Kurnool, (Andhra Pradesh), India
[2]Jr. Lecturer in Maths, Govt Jr College, Kurnool, (Andhra Pradesh), India

(Corresponding author: K. Gayathri Devi)
(Received 07 April 2019, Revised 26 June 2019 Accepted 09 July 2019)
(Published by Research Trend, Website: www.researchtrend.net)

ABSTRACT: In this paper, we try to study the heat transfer flow by natural convection and radiation with variable wall temperature in a saturated porous medium confined in a rectangular cavity. In this study we assume the left vertical wall of the cavity is at temperature T_h (T_h+By^{λ}) and right vertical wall temperature T_c (T_h>T_c) the top and bottom horizontal surfaces of the cavity are adiabatic. Darcy law is to be obeyed to the flow inside the porous medium the properties of the fluid and porous medium are homogeneous, isotropic and constant expect variation of fluid density with temperature. The fluid and porous medium are in thermal equilibrium and flux of heat radiation in y - direction is negligible in comparison to that in x-direction. Galerkin Finite Element Method of three nodded triangular elements has been used to convert the partial differential equations into the matrix form equations. Results are presented in terms of stream functions and isotherms for various values of Aspect ratios, Radiation parameters, Rayleigh numbers, Nusselt numbers and Power law exponents(λ).

Keywords: Convective Heat Flow, Rectangular Cavity, Non-Isothermal Wall, natural convection, Radiation parameters, Rayleigh numbers

I. INTRODUCTION

The study of natural convection heat transfer in confined saturated porous medium with a fluid has important engineering applications such as Geothermal systems, Nuclear engineering, Petroleum engineering and Insulation technology etc.

A natural convection, in a vertical rectangular cavity filled with a non-Newtonian fluid and subjected to uniform heat flux along the vertical side walls, is carried out numerically by solving the full governing equations. In the limit of a tall enclosure, these equations are considerably reduced by using the parallel flow approximation. Solutions for the flow and temperature fields, and the heat transfer rate, are obtained as functions of the governing parameters. Good agreement is found between the results of the two approaches for a wide range of governing parameters.

The natural convective heat transfer of pseudoplastic fluids in a square cavity with a heated bottom and cooled top walls was examined by a direct numerical analysis using the Sutterby model. Consequently, it could be verified that the heat transfer rate of pseudoplastic fluids became larger than that of a Newtonian fluid under thermal conditions where stable vortex flows were formed. The reason is that fluid flows are easy to further develop particularly near the walls due to the decrease in the apparent viscosity by the shear-thinning effect. On the other hand, it was found that the locally larger change in viscosity had the potential of causing the formation of a complicated flow field when the non-Newtonian fluid was highly pseudoplastic and the Rayleigh number increased. The contribution of the shear-thinning effect depending on the non-Newtonian property and the thermal condition was clearly revealed. Darcy's law is the equation that defines the ability of a fluid to flow through a porous media such as rock. It relies on the principle that the amount of flow between two points is directly proportional to the difference in pressure between the points and the ability of the media through which it is flowing to impede the flow. Here pressure refers to the excess of local pressure over the normal hydrostatic fluid pressure which, due to gravity, increases with depth like in a standing column of water. This factor of flow impedance is referred to as permeability.

Darcy's law is a simple proportional relationship between the instantaneous discharge rate through a porous medium and the pressure drop over a given distance.

Darcy's law is usually written as:

$$Q = -KA\, dh/dl$$

where : Q = rate of water flow (volume per time)
K = hydraulic conductivity
A = column cross sectional area
dh/dl = hydraulic gradient, that is, the change in head over the length of interest.

The literature, natural convection heat Transfer in enclosures by Ostrach [1]. Unsteady natural convection in a rectangular cavity by Patterson [2], Applied Finite element analysis by Segerland [3] is inspired in research. An experimental investigation of mixed cavity natural convection in the high Rayleigh number regime by Kirkpatrick [4], Natural convection in rectangular enclosures from below and cooled along one side explained detailed by November *et.al.,* [5].
Transient natural convection in a rectangular enclosure with one heated side wall by Hall and Bejan [6] Heat transfer in square cavities with partially active vertically walls numerically explained by Valencia and Frederick [7].

Numerical solutions of transient natural convection in a square cavity with different side wall temperature and Natural convection in a differentially heated square cavity with internal heat generation are given by Hyun *et.al.,* [8], Natural convection in rectangular enclosures heated from below and symmetrically cooled from the sides numerically explained by Milanez [9], Cheung etal..[10] Problems in Isotropic Seepage by Finite Elements are solved numerically. Natural convection in rectangular enclosures heated from one side and cooled from the ceiling investigated by Ayhan [11], Free Convection in a Thermally Stratified Non-Darcy Porous Medium Saturated with a Non-Newtonian Fluid, P.V.S.N. Murthy [12], Forced Convection Flow of Power-Law Fluids Over a Flat Plate Embedded in a Darcy-Brinkman Porous Medium Asterios and Eugun [13], A numerical study on natural convection in porous media-filled an inclined triangular enclosure with heat sources using nano-fluid in the presence of heat generation effect by Mansour and Ahmed [14], The flow of a rarefied gas in a rectangular enclosure due to the non-isothermal walls with no synergetic contributions from external force fields is investigated by Stefanov [15]. The radiant efflux from a cylindrical cavity having non-isothermal bounding surfaces is determined by solving a problem of combined radiation and conduction by Heinisch [16], Combined effects of thermal radiation and internal heat source/sink, formulation for natural-convection flow in a square cavity filled with porous medium using isothermal vertical walls and adiabatic horizontal ones, has been studied numerically by using finite-difference technique in staggered grid distribution by Sabyasachi *et al.,* [17].

II. MATHEMATICAL FORMULATION

Consider a two dimensional cavity of height and width (L) filled with saturated porous medium, the left vertical surface of the cavity is maintained at temperature T_h greater than right vertical surface temperature T_c, the top and bottom horizontal surfaces of the cavity are adiabatic. The flow inside the porous medium is assumed to obey Darcy law and there is no phase changes of the fluid the properties of the fluid and porous medium are homogeneous, isotropic and constant except variation of fluid density with temperature. The fluid and porous medium are in thermal equilibrium and radiative heat flux in y direction is negligible in comparison to that in the x - direction.

The governing equations in Cartesian Coordinates can be written as

$$\frac{\partial u}{\partial x} + \frac{\partial v}{\partial y} = 0 \qquad (1)$$

$$\frac{\partial v}{\partial x} \quad \frac{\partial u}{\partial y} = \frac{gK\beta}{v}\frac{\partial T}{\partial x} \qquad (2)$$

$$u\frac{\partial T}{\partial x} + v\frac{\partial T}{\partial y} = \alpha\left[\left(\frac{\partial^2 T}{\partial x^2} + \frac{\partial^2 T}{\partial y^2}\right)\right] + \frac{1}{\rho c_p}\frac{4n^2\sigma}{3\beta_R}\frac{\partial^2 T^4}{\partial x^2} \qquad (3)$$

With the boundary conditions are

At hot wall $x = 0$ $u = 0, v = 0$ $T = T_\infty + B\,y^\lambda$

At cold wall $x = L$ $u = 0, v = 0$ $T = T_c$

At hot wall $y = 0$ $u = 0, v = 0$ $\frac{\partial T}{\partial y} = 0$

At cold wall $y = L$ $u = 0, v = 0$ $\frac{\partial T}{\partial y} = 0$

The Continuity equation (1) can be satisfied automatically by introducing the stream function 'ψ' as

$$u = \frac{\partial \psi}{\partial y} \qquad (4.a)$$

$$v = \frac{\partial \psi}{\partial x} \qquad (4.b)$$

where x and y are the distances measured along the horizontal and vertical directions respectively and u and v are the velocity components in the x - and y - directions respectively.

Using the following non dimensional variables,

Width, $X = \frac{x}{L}$ Height, $Y = \frac{y}{L}$ and Stream function, $\bar{\psi} = \frac{\psi}{\alpha}$

The governing equations (1) to (3) reduced to non-dimensional form and introducing stream function 'ψ'

$$\frac{\partial^2 \bar{\psi}}{\partial X^2} + \frac{\partial^2 \bar{\psi}}{\partial Y^2} = Ra\frac{\partial \theta}{\partial X} \qquad (5)$$

$$\left[\frac{\partial \bar{\psi}}{\partial Y}\frac{\partial \theta}{\partial X} \quad \frac{\partial \bar{\psi}}{\partial X}\frac{\partial \theta}{\partial Y}\right] = \left(\left(1 + \frac{4R_d}{3}\right)\frac{\partial^2 \theta}{\partial X^2} + \frac{\partial^2 \theta}{\partial Y^2}\right) \qquad (6)$$

Where T denotes the temperature ϑ and α are kinematic viscosity and thermal diffusivity respectively, K is the medium permeability, T_h and T_c are the temperatures at hot bottom wall and cold vertical walls respectively L is the side of the square cavity.

Temperature $\theta = \frac{T \quad T_\infty}{T_W \quad T_\infty}$

Radiation Parameter $R_d = \frac{4\sigma n^2 T_\infty^3}{\beta_R K_S}$

Rayleigh number $Ra = \frac{g\beta_T \Delta TKL}{v\alpha}$

With the non-dimensionless boundary conditions are

at X = 0 $\bar{\psi} = 0$ $\theta = 1$

at X = 1 $\bar{\psi} = 0$ $\theta = 1$

at Y = 0 $\bar{\psi} = 0$ $\frac{\partial \theta}{\partial y} = 0$

at Y = 1 $\bar{\psi} = 0$ $\frac{\partial \theta}{\partial y} = 0$

III. SOLUTION OF THE PROBLEM

Thus far we have derived the partial differential equations, which describe the heat and fluid flow behavior in the vicinity of porous medium. The development of governing equations is one part but the second and important part is to solve these equations in order to predict the various parameters of interest in the porous medium. There are various numerical methods available to achieve the solution of these equations, but the most popular numerical methods are Finite difference method, Finite volume method and the Finite element method. The selection of these numerical methods is an important decision, which is influenced by variety of factors amongst which the geometry of domain plays a vital role. Other factors include the ease with which these partial differential equations can be transformed into simple forms, the computational time required and the flexibility in development of computer code to solve these equations.

In the present study, we have predominantly used Finite Element Method (FEM). The following sections enlighten the Finite element method and present its application to solve the governing equations.

The Finite Element Method is a deservingly popular method amongst scientific community. This method was originally developed to study the mechanical stresses in a complex air frame structure popularized by Zienkiewicz and Cheung by applying it to continuum mechanics. Since the application of Finite Element Method has been exploited to solve the number of problems in various engineering disciplines. The great thing about finite element method is its ease with which it can be generalized to myriad engineering problems comprised of different materials.

Another admirable feature of the Finite Element Method (FEM) is that it can be applied wide range of geometries having irregular boundaries, which is highly difficult to achieve with other contemporary methods. FEM can be said to have comprised of roughly 5 steps to solve any particular problem.

The steps can be summarized as

- **Descritizing the domain:** This step involves the division of whole physical domain into smaller segments known as elements, and then identifying the nodes, coordinates of each node and ensuring proper connectivity between the nodes.
- **Specifying the equation:** In this step, the governing equation is specified and an equation is written in terms of nodal values.
- **Development of Global matrix:** The equations are arranged in a global matrix which takes into account the whole domain.
- **Solution:** The equations are solved to get the desired variable at each table in the domain.
- **Evaluate the quantities of interest:** After solving the equations a set of values is obtained for each node, which can be further processed to get the quantities of interest.

There are varieties of elements available in FEM, which are distinguished by the presence of number of nodes. The present study is carried out by using a simple 3-noded triangular element.

Good insight into the FEM Galerkin method is employed to convert the partial differential equations into matrix form for an element. The steps invented are as given below. Please note that the nodal terms *i, j & k* are replaced by 1, 2 & 3 respectively in subsequent discussions for simplicity.

The momentum and energy balance equations are solved using the Galerkin finite element method. Continuity equation will be used as a constraint due to mass conservation and this constraint may be used to obtain the pressure distribution. In order to solve equations, we use the finite element method where the pressure P is eliminated by a penalty parameter γ and the incompressibility criteria given by equation (1) which results in

$$P = \gamma\left(\frac{\partial U}{\partial X}+\frac{\partial V}{\partial Y}\right)$$

The continuity equation (1) is automatically satisfied for large values of γ.

Application of Galerkin method to equation (5) yields

$$\left\{R^e\right\} = \int_A N^T\left(\frac{\partial^2\bar{\psi}}{\partial\bar{x}^2}+\frac{\partial^2\bar{\psi}}{\partial\bar{y}^2}+Ra\frac{\partial\bar{T}}{\partial\bar{x}}\right)dA \qquad (7)$$

where R^e is the residue. Considering individual terms of equation (7), the differentiation of following terms results into

$$\frac{\partial}{\partial X}\left([N]^T\frac{\partial\bar{\psi}}{\partial X}\right)=[N]^T\frac{\partial^2\bar{\psi}}{\partial X^2}+\frac{\partial[N]^T}{\partial X}\frac{\partial\bar{\psi}}{\partial X} \qquad (8)$$

Thus

$$\int_A N^T\frac{\partial^2\bar{\psi}}{\partial X^2}dA=\int_A\frac{\partial}{\partial X}\left([N]^T\frac{\partial^2\bar{\psi}}{\partial X^2}\right)dA \quad \int_A\frac{\partial[N]^T}{dX}\frac{\partial\bar{\psi}}{\partial X} \qquad (9)$$

The first term on right hand side of equation (9) can be transformed into surface integral by the application of Greens theorem and leads to inter-element requirement at boundaries of an element. The boundary conditions are incorporated in the force vector.

Making use of $T = N_i T_i + N_j T_j + N_k T_k$

$$\int_A N^T\frac{\partial^2\bar{\psi}}{\partial X^2}dA=\int_A\frac{\partial N^T}{dX}\frac{\partial N}{\partial X}\begin{Bmatrix}\bar{\psi}_1\\ \bar{\psi}_2\\ \bar{\psi}_3\end{Bmatrix}dA \qquad (10)$$

Substitution of $N_m=\frac{a_m+b_m+c_m y}{2a}$, m = i, j, k into equation (10)

$$= \frac{1}{(2A)^2}\int_A\begin{bmatrix}b_1\\ b_2\\ b_3\end{bmatrix}[b_1b_2b_3]\begin{Bmatrix}\bar{\psi}_1\\ \bar{\psi}_2\\ \bar{\psi}_3\end{Bmatrix}dA$$

$$= \frac{1}{4A}\begin{bmatrix}b^2 & b_1b_2 & b_1b_3\\ b_1b_2 & b_2^2 & b_2b_3\\ b_1b_3 & b_2b_3 & b_3^2\end{bmatrix}\begin{Bmatrix}\bar{\psi}_1\\ \bar{\psi}_2\\ \bar{\psi}_3\end{Bmatrix} \qquad (11)$$

Similarly $\int_A N^T\frac{\partial^2\bar{\psi}}{\partial X^2}dA=\frac{1}{4A}\begin{bmatrix}c_1^2 & c_1c_2 & c_1c_3\\ c_1c_2 & c_2^2 & c_2c_3\\ c_1c_2 & c_2c_3 & c_3^2\end{bmatrix}\begin{Bmatrix}\bar{\psi}_1\\ \bar{\psi}_2\\ \bar{\psi}_3\end{Bmatrix}$ (12)

The third term of the equation (7) is

$$\int_A N^T Ra\frac{\partial\theta}{\partial X}dA=Ra\int_A N^T\frac{\partial\theta}{\partial X}dA \qquad (13)$$

In order to get the matrix equation of (13) the triangular elements can be subdivided into three triangles with a point in the center of original triangles, replace shape functions and using the area integration like first problem.

We get

$$= Ra\frac{A}{3}\begin{bmatrix}1\\1\\1\end{bmatrix}\frac{1}{2A}b_1+b_2+b_3\begin{bmatrix}\theta_1\\ \theta_2\\ \theta_3\end{bmatrix}$$

$$= \frac{Ra}{6}\begin{Bmatrix}b_1\theta_1+b_2\theta_2+b_3\theta_3\\ b_1\theta_1+b_2\theta_2+b_3\theta_3\\ b_1\theta_1+b_2\theta_2+b_3\theta_3\end{Bmatrix} \qquad (14)$$

The equation (7) can be written in the matrix form as:

$$=\frac{1}{4A}\left\{\begin{bmatrix} b^2 & b_1b_2 & b_1b_3 \\ b_1b_2 & b_2^2 & b_2b_3 \\ b_1b_3 & b_2b_3 & b_3^2 \end{bmatrix}+\begin{bmatrix} c_1^2 & c_1c_2 & c_1c_3 \\ c_1c_2 & c_2^2 & c_2c_3 \\ c_1c_2 & c_2c_3 & c_3^2 \end{bmatrix}\right\}\begin{Bmatrix}\bar{\psi}_1\\ \bar{\psi}_2\\ \bar{\psi}_3\end{Bmatrix}=\frac{Ra}{6}\begin{Bmatrix} b_1\theta_1+b_2\theta_2+b_3\theta_3 \\ b_1\theta_1+b_2\theta_2+b_3\theta_3 \\ b_1\theta_1+b_2\theta_2+b_3\theta_3 \end{Bmatrix} \quad (15)$$

The Finite Element Method of the Energy Equation

$$\{R^e\}=\int_A [N]^T\left[\left(\frac{\partial\bar{\psi}}{\partial Y}\frac{\partial\theta}{\partial X}\quad \frac{\partial\bar{\psi}}{\partial X}\frac{\partial\theta}{\partial Y}\right)\quad\left(\left(1+\frac{4R_d}{3}\right)\frac{\partial^2\theta}{\partial X^2}+\frac{\partial^2\theta}{\partial Y^2}\right)\right]dA \quad (16)$$

Considering the terms individually,

$$\int_A [N]^T\frac{\partial\bar{\psi}}{\partial Y}\frac{\partial\theta}{\partial X}dA=\int_A\begin{bmatrix}L_1\\L_2\\L_3\end{bmatrix}\frac{\partial[N]}{\partial Y}\{\bar{\psi}\}\frac{\partial[N]}{\partial X}\{\theta\}dA \quad (17)$$

$$=\int_A\begin{bmatrix}L_1\\L_2\\L_3\end{bmatrix}dA\ \frac{1}{4A^2}\left[c_1\bar{\psi}_1+c_2\bar{\psi}_2+c_3\bar{\psi}_3\right]\ [b_1,b_2,b_3]\begin{bmatrix}\theta_1\\\theta_2\\\theta_3\end{bmatrix} \quad (18)$$

$$=\frac{1}{12A}\begin{Bmatrix}c_1\bar{\psi}_1+c_2\bar{\psi}_2+c_3\bar{\psi}_3\\ c_1\bar{\psi}_1+c_2\bar{\psi}_2+c_3\bar{\psi}_3\\ c_1\bar{\psi}_1+c_2\bar{\psi}_2+c_3\bar{\psi}_3\end{Bmatrix}[b_1,b_2,b_3]\begin{bmatrix}\theta_1\\\theta_2\\\theta_3\end{bmatrix} \quad (19)$$

Similarly $\int_A N^T\frac{\partial\bar{\psi}}{\partial X}\frac{\partial\theta}{\partial Y}dA=\frac{1}{12A}\begin{Bmatrix}b_1\bar{\psi}_1+b_2\bar{\psi}_2+b_3\bar{\psi}_3\\ b_1\bar{\psi}_1+b_2\bar{\psi}_2+b_3\bar{\psi}_3\\ b_1\bar{\psi}_1+b_2\bar{\psi}_2+b_3\bar{\psi}_3\end{Bmatrix}[c_1,c_2,c_3]\begin{bmatrix}\theta_1\\\theta_2\\\theta_3\end{bmatrix}$ (20)

The remaining two terms of energy equation are evaluated as

$$\int_A N^T\left[1+\frac{4}{3}R_d\right]\frac{\partial^2\theta}{\partial X^2}dA=\frac{1}{4A}\left(1+\frac{4R_d}{3}\right)\begin{bmatrix}b_1^2 & b_1b_2 & b_1b_3\\ b_1b_2 & b_2^2 & b_2b_3\\ b_1b_3 & b_2b_3 & b_3^3\end{bmatrix}\begin{bmatrix}\theta_1\\\theta_2\\\theta_3\end{bmatrix} \quad (21)$$

$$\int_A N^T\frac{\partial^2\theta}{\partial Y^2}dA=\frac{1}{4A}\begin{bmatrix}c_1^2 & c_1c_2 & c_1c_3\\ c_1c_2 & c_2^2 & c_2c_3\\ c_1c_3 & c_2c_3 & c_3^2\end{bmatrix}\begin{bmatrix}\theta_1\\\theta_2\\\theta_3\end{bmatrix} \quad (22)$$

Thus the stiffness matrix is given by

$$\frac{1}{12A}\begin{Bmatrix}c_1\bar{\psi}_1+c_2\bar{\psi}_2+c_3\bar{\psi}_3\\ c_1\bar{\psi}_1+c_2\bar{\psi}_2+c_3\bar{\psi}_3\\ c_1\bar{\psi}_1+c_2\bar{\psi}_2+c_3\bar{\psi}_3\end{Bmatrix}[b_1,b_2,b_3]\ \frac{1}{12A}\begin{Bmatrix}b_1\bar{\psi}_1+b_2\bar{\psi}_2+b_3\bar{\psi}_3\\ b_1\bar{\psi}_1+b_2\bar{\psi}_2+b_3\bar{\psi}_3\\ b_1\bar{\psi}_1+b_2\bar{\psi}_2+b_3\bar{\psi}_3\end{Bmatrix}[c_1,c_2,c_3]$$

$$+\frac{1}{4A}\left(\left[1+\frac{4}{3}R_d\right]\begin{bmatrix}b_1^2 & b_1b_2 & b_1b_3\\ b_1b_2 & b_2^2 & b_2b_3\\ b_1b_3 & b_2b_3 & b_3^2\end{bmatrix}+\begin{bmatrix}c_1^2 & c_1c_2 & c_1c_3\\ c_1c_2 & c_2^2 & c_2c_3\\ c_1c_3 & c_2c_3 & c_3^2\end{bmatrix}\right)\begin{bmatrix}\theta_1\\\theta_2\\\theta_3\end{bmatrix}=0 \quad (23)$$

Nusselt Number

The dimensionless average Nusslet number ($\overline{Nu}$) can be calculated using the formula

$$\overline{Nu}=\int_0^1 Nu_Y dY \quad (24)$$

Where $Nu_Y=-\left[\left(1+\frac{4R_d}{3}\right)\frac{\partial\theta}{\partial X}\right]_{X=0,1}$

IV. RESULTS AND DISCUSSION

The effect of λ on Streamlines and Isotherms of the fluid is illustrated in fig (1) and Fig. (2), which corresponds to the values Ra = 50, A_r = 1, and R_d = 1 and Ra = 100, A_r = 1 and R_d = 1 respectively. In both figures the magnitude of the streamlines decreases when λ increases from 0 to 1 is and streamlines tend to move towards upper horizontal wall. In isotherms thickness of the thermal boundary layer becomes small with increase in λ.

The effect of Ra on Stream lines and Isotherms of the fluid is illustrated in Fig. 3 and 4, which corresponds to the values, λ = 0.25, A_r = 1, and R_d = 1 and λ = 1, A_r = 1 and R_d = 1 respectively. In both figures the increased Raleigh numbers is associated with higher convection heat transfer thus the streamlines crowded and covers almost whole domain. In both cases the area occupied by the temperature lines decreases when Ra is maximum.

The effect of A_r on Stream lines and Isotherms of the fluid is illustrated in Fig. (5) and Fig. (6), which corresponds to the values, Ra = 100 λ = 0.25 and R_d = 3 and λ = 1, Ra = 100 and R_d = 3 respectively. In both cases with increase in A_r the streamlines are distorted and crowded near upper horizontal wall of the cavity, indicating the increasing fluid velocity at that position. Particularly near A_r = 2 we observe convective effect is observed at lower left, upper right corners of the cavity, in Fig.(6), but it shift into upper portion of the hot wall in figure (6).

The effect of R_d on Stream lines and Isotherms of the fluid is illustrated in Fig. 7 and 8, which corresponds to the values, Ra = 100, A_r = 1, λ = 0.25, and and λ = 1, Ra = 100 and A_r = 1 respectively In both cases we observe from the streamlines that the flow consists of a single cell and it is clear from the streamlines that the velocity of the fluid increases with increase in R_d form isotherms we conclude that the thermal boundary layer become thin.

GRAPHS:

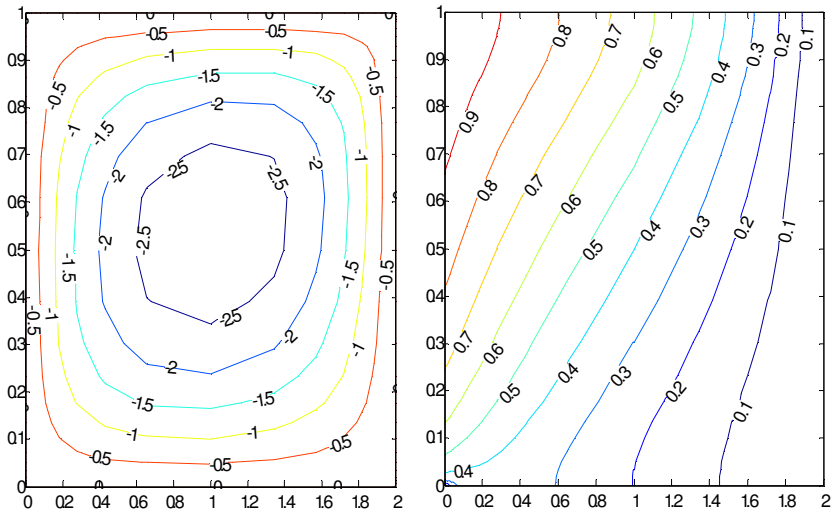

(a)

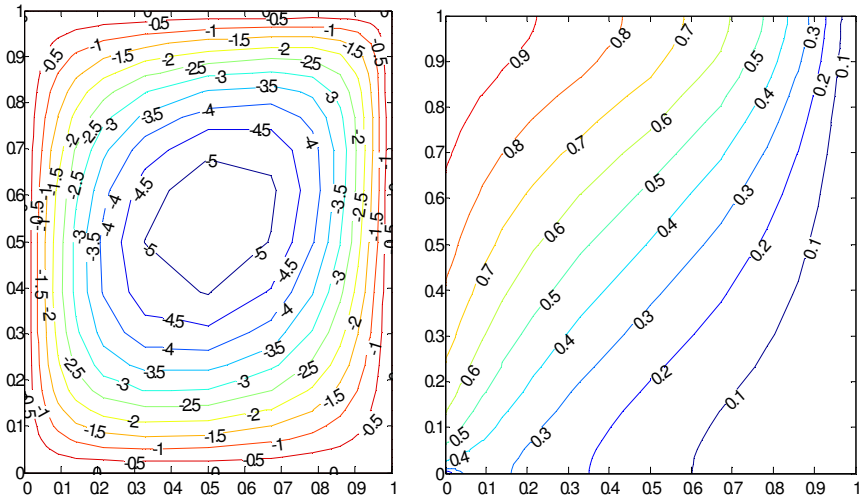

(b)

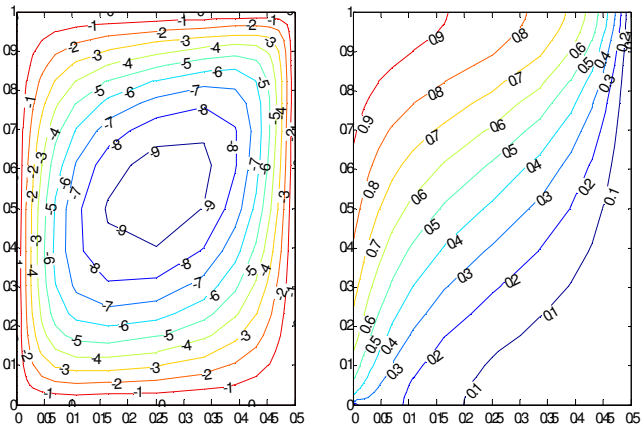

(c)

Fig. 1. Streamlines (Left) and Isotherms (Right) for Ra = 100, R_d = 3, λ=0.25
a) A_r =0.5 b) A_r =1 c) A_r =2.

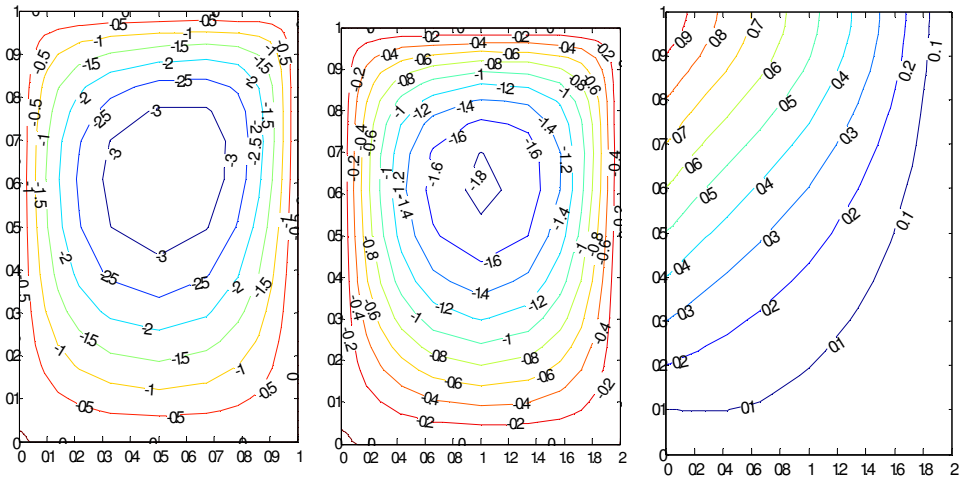

(a) (b)

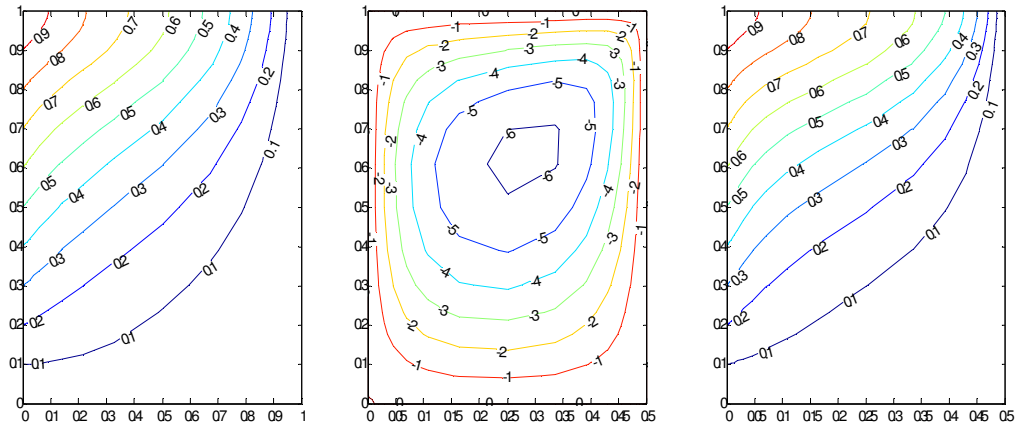

(c)

Fig. 2. Streamlines (Left) and Isotherms (Right) for Ra=100, R_d =3, λ=1
(a) A_r = 0.5 (b) A_r = 1 (c) A_r = 2.

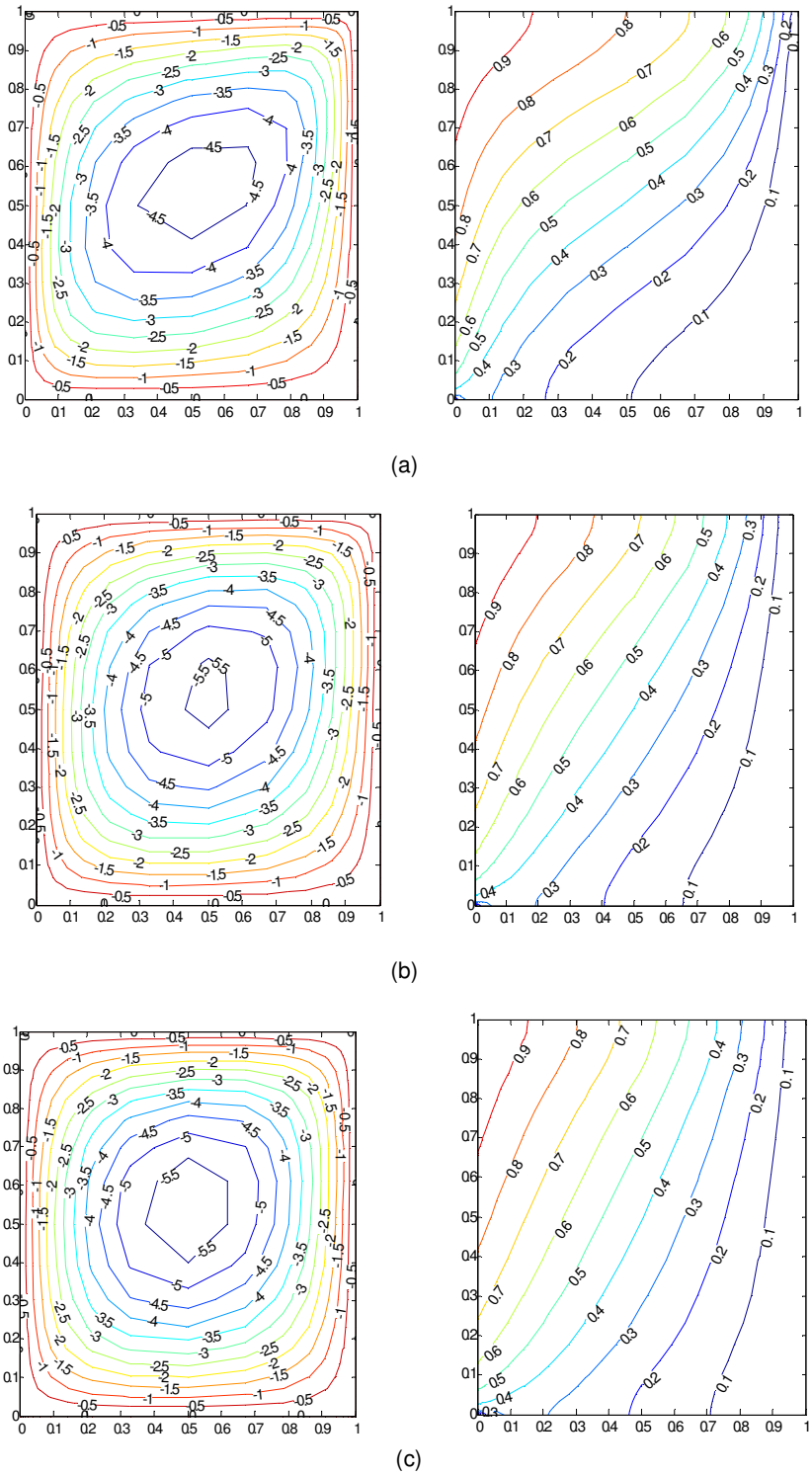

Fig. 3. Streamlines (Left) and Isotherms (Right) for Ra = 100, A_r = 1, λ=0.25
(a) R_d = 1 (b) R_d = 5 (c) R_d = 10.

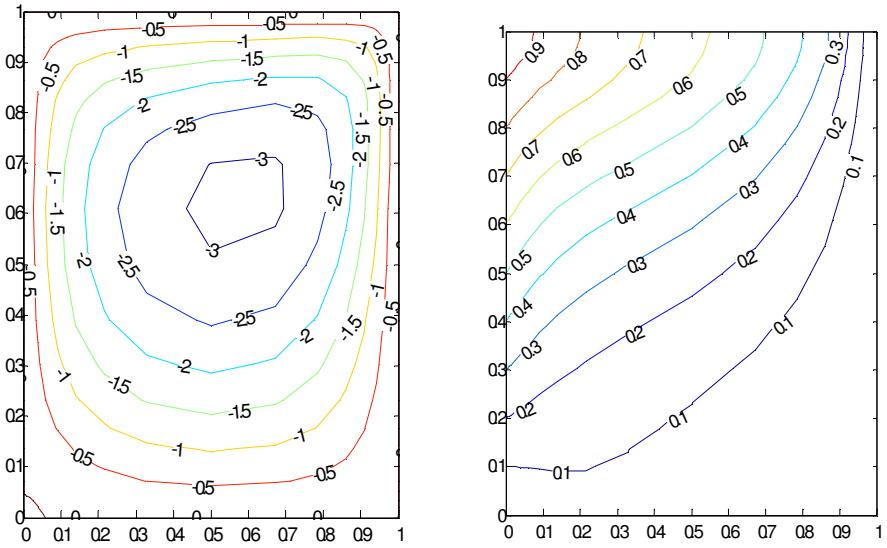

(a)

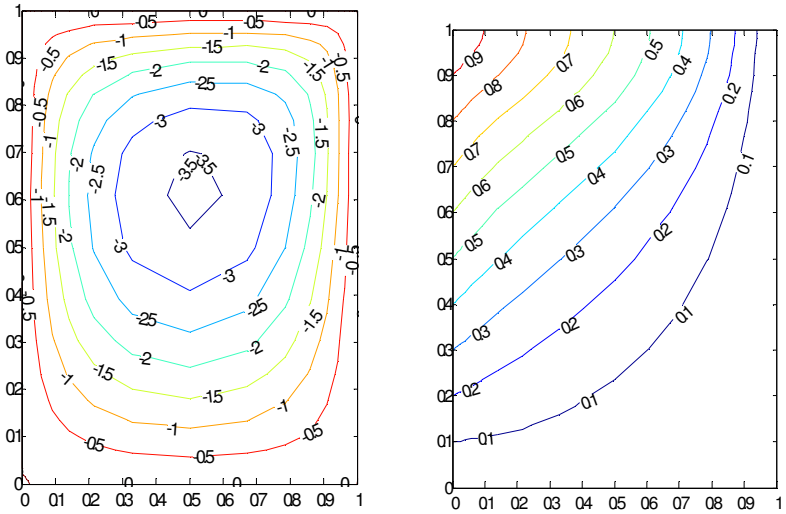

(b)

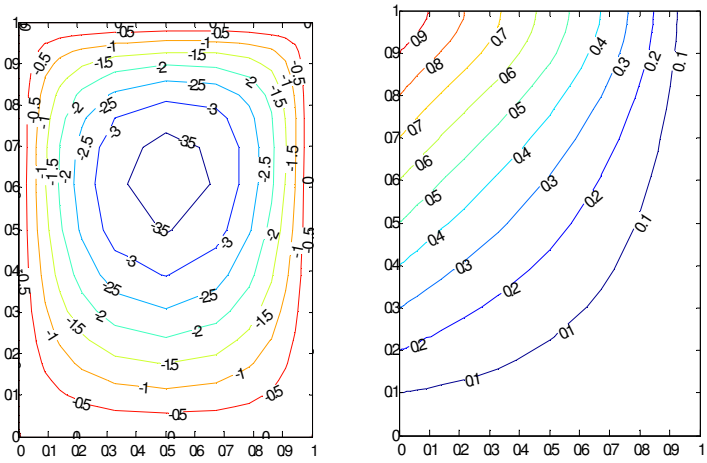

(c)

Fig. 4. Streamlines (Left) and Isotherms (Right) for Ra =100, A_r = 1, λ = 1
(a) R_d = 1 (b) R_d = 5 (c) R_d = 10.

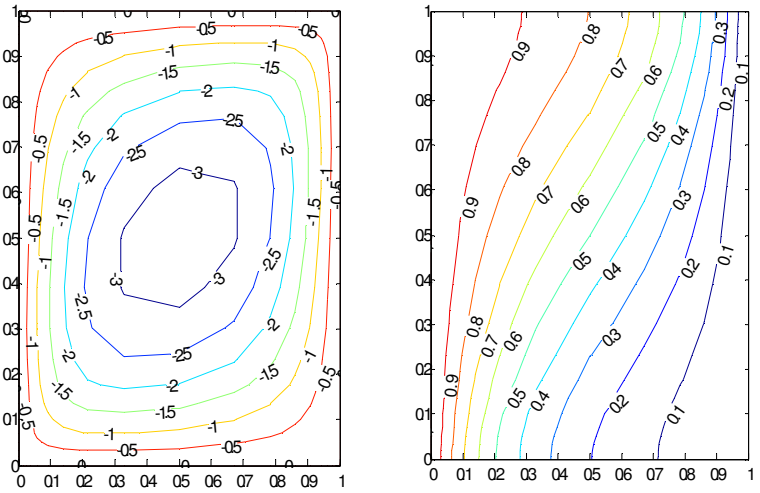

(a)

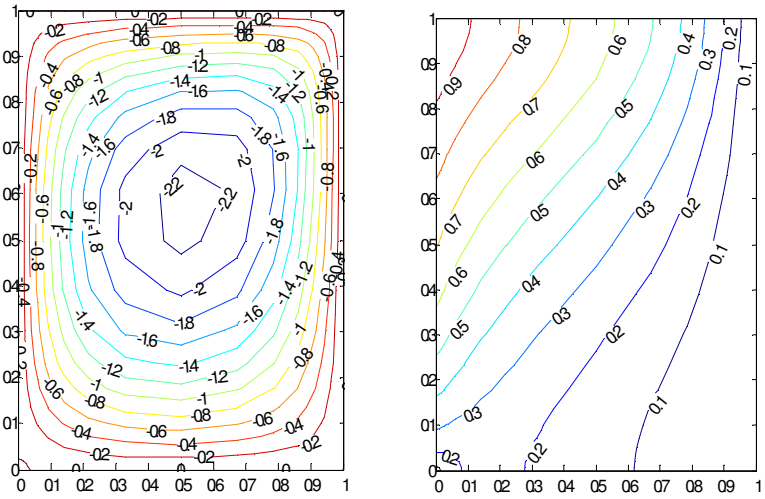

(b)

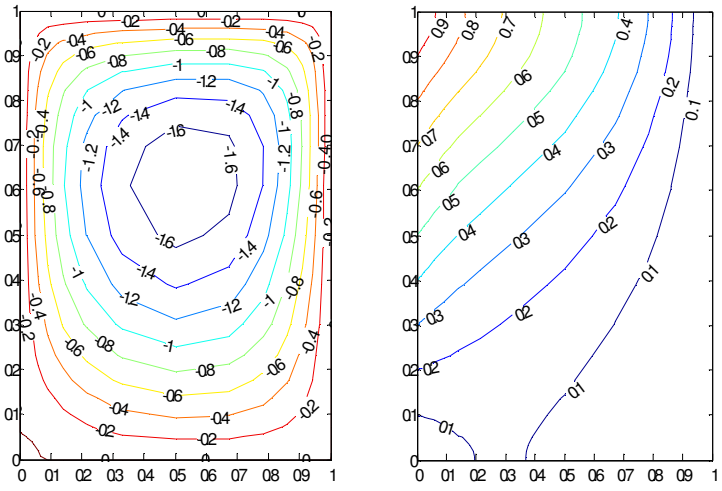

(c)

Fig. 5. Streamlines (Left) and Isotherms (Right) for Ra=50, A_r =1, R_d =1
a) λ=0 b) λ=0.5 c) λ=1.

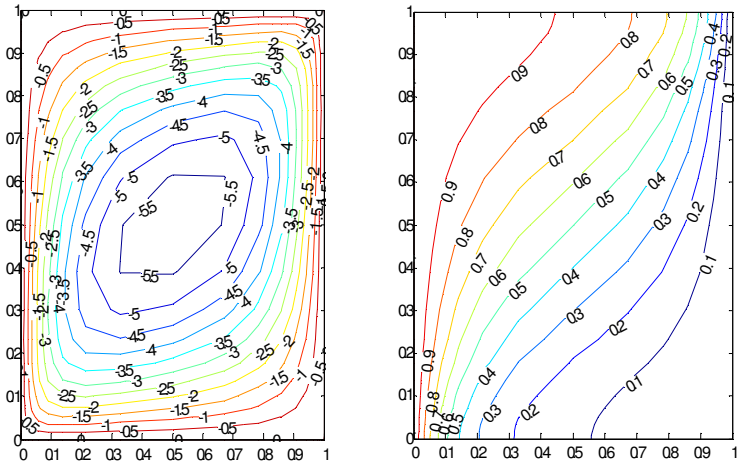

a)

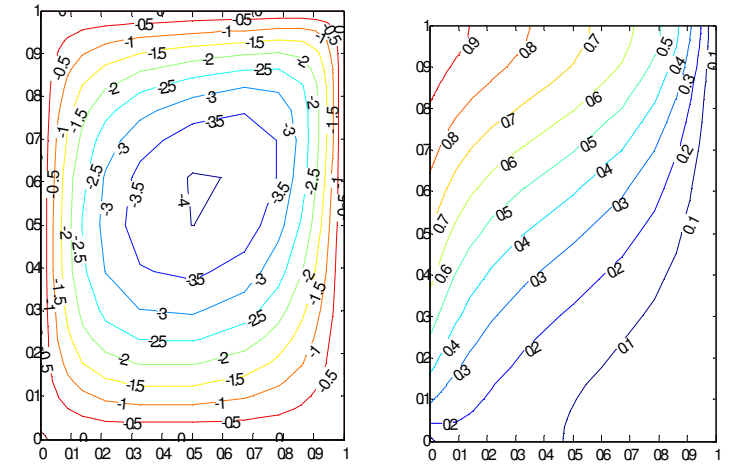

b)

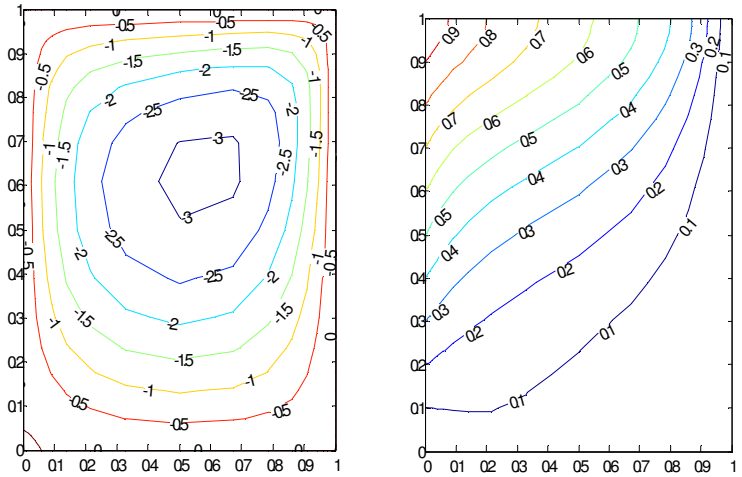

c)

Fig. 6. Streamlines (Left) and Isotherms (Right) for Ra=100, A_r =1, R_d =1
a) λ=0 b) λ=0.5 c) λ=1.

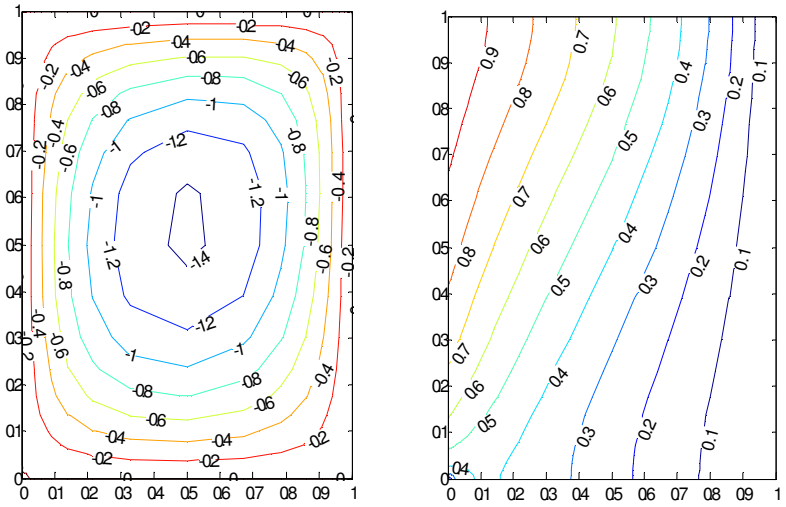

a)

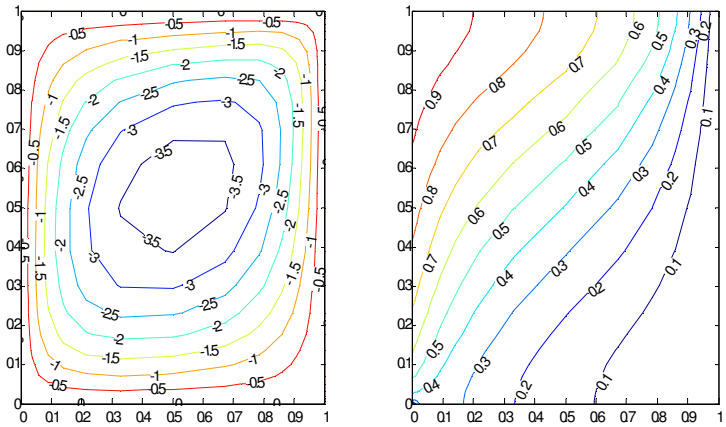

b)

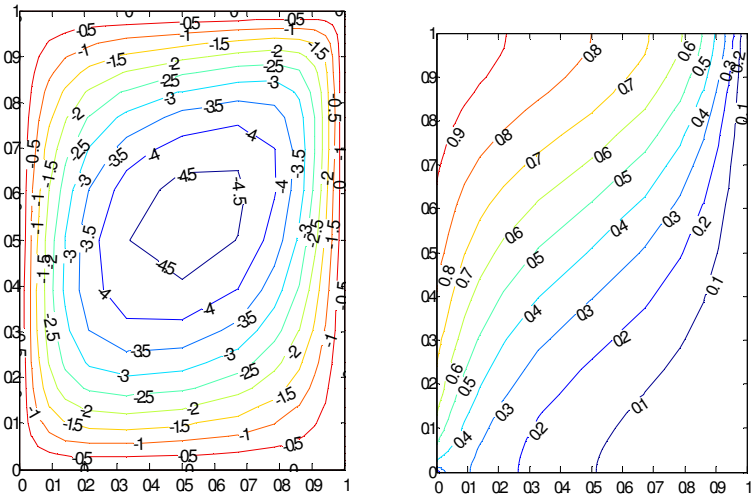

c)

Fig. 7. Streamlines (Left) and Isotherms (Right) for A_r =1,R_d =1, λ=0.25
a) Ra=25 b) Ra=75 c) Ra=100.

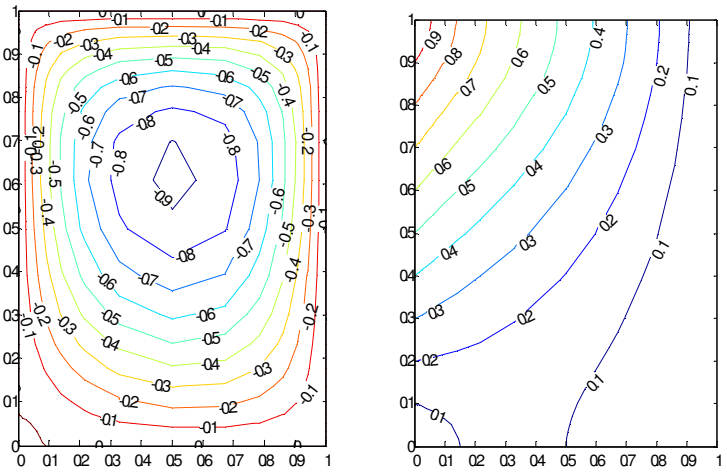

a)

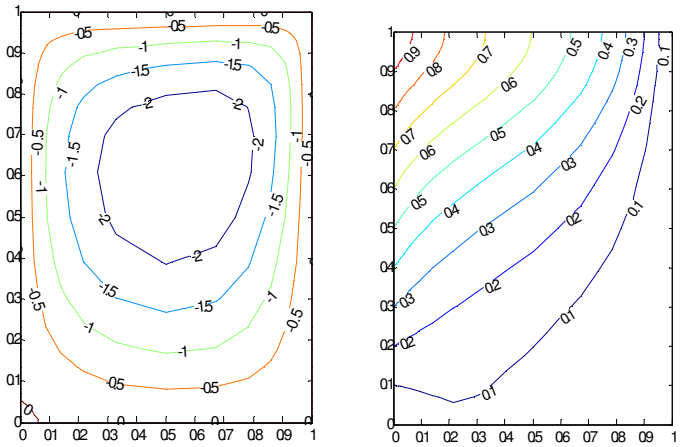

b)

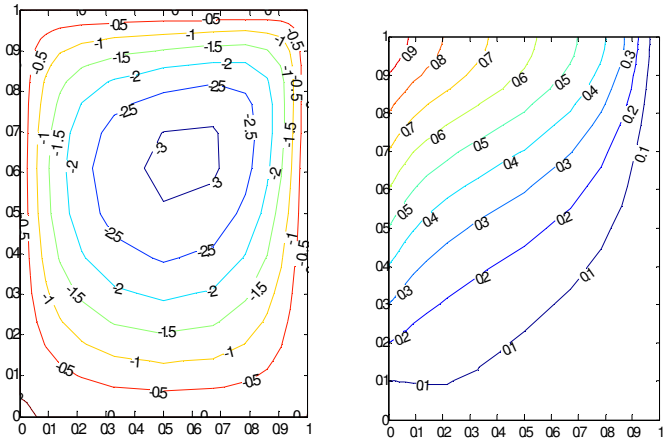

c)

Fig. 8. Streamlines (Left) and Isotherms (Right) for A_r =1,R_d =1, λ=1
a) Ra=25 b) Ra=75 c) Ra=100.

Fig. 9 shows the variation of $\bar{N}u$ with respect to A $_r$ of the cavity for various values of power law exponent at R_d = 3, Ra = 100.The $\bar{N}u$ is higher for the case of isothermal wall temperature. For a given value of Ar the lines corresponds to λ>0 come close in between A_r, 0.5 to 1 but it changes with increase in A_r.

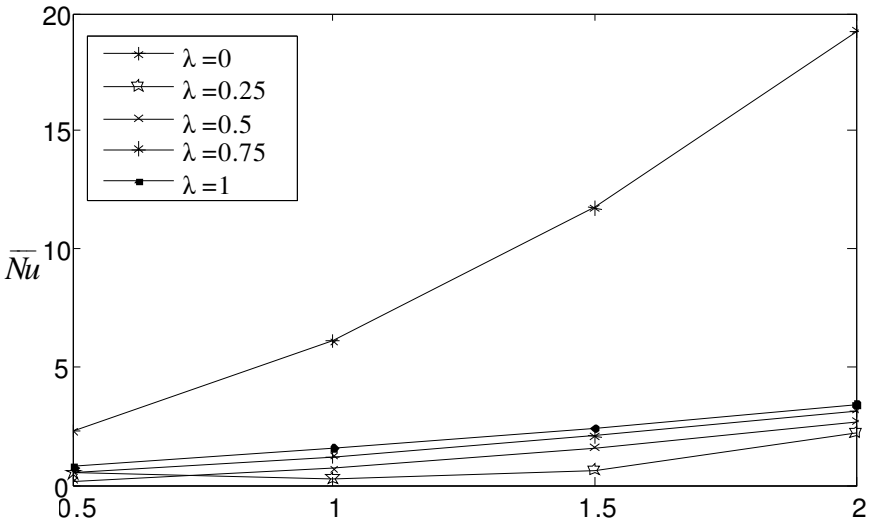

Fig. 9. $\bar{N}u$Variations with Ar at hot surface for different values of λ at Rd =3, Ra=100.

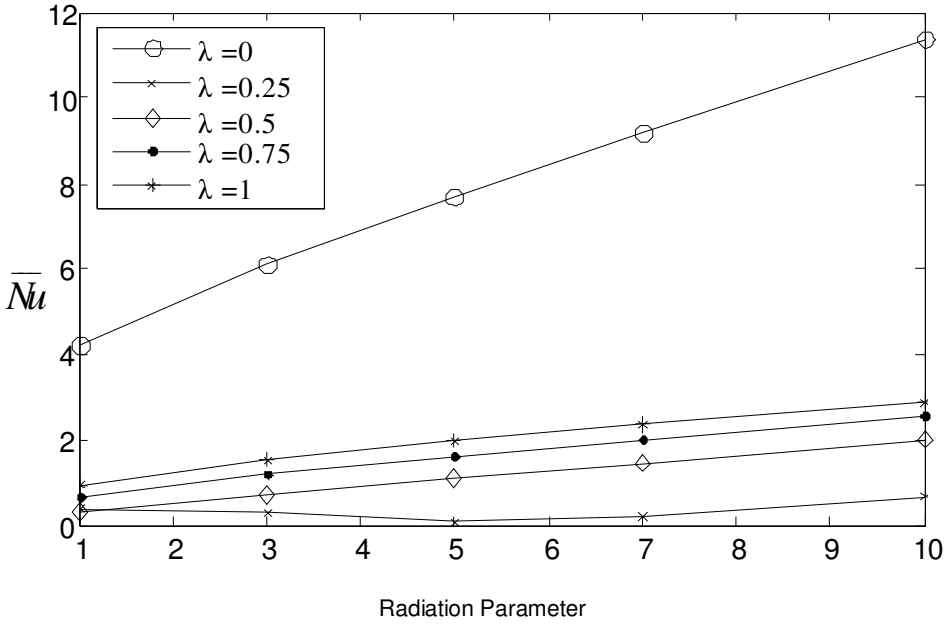

Fig. 10. $\bar{N}u$ Variations with R_d at hot surface for different values of λ at A_r =1, Ra=100.

Fig.10 shows the variation of $\bar{N}u$ with respect to R_d for variation values of λ at A_r = 1, Ra = 100. $\bar{N}u$ Increases with increase in R_d except at λ = 1. But the line corresponds to λ = 1 first gradually decreases next it increases with increase in R_d. It is clear from the figure that heat content of the wall is more at λ = 0, compared with other values of λ.

Fig. 11 shows the variation of $\bar{N}u$ with respect to Ra for various values of A_r at λ = 1, R_d = 3. $\bar{N}u$ Increases with increase in A_r. By comparing the lines corresponds to A_r = 0.5, A_r = 2 the effective change is observed.

Fig. 12 shows the variation of $\bar{N}u$ with respect to Ra for various values of R_d at λ = 1, Ar = 1.It is clear from the figure that increase in $\bar{N}u$ is almost linear with respect to Ra.

Fig. 13 shows the variation of $\bar{N}u$ with respect to λ for hot surface at various values of Ra at A_r = 1, R_d = 1. It is obvious from the figure that the line corresponds to different Ra decreases with increase in λ, but they merge two times in between λ = 0.1 to 0.5 and next they increases with increase in λ. But all the lines come close at high value of λ.

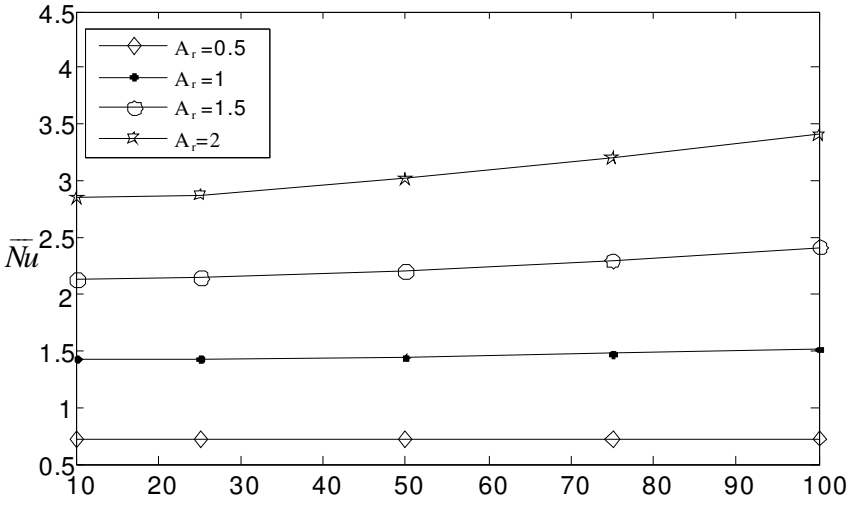

Fig. 11. $\bar{N}u$ Variations with Ra at hot surface for different values of A_r at λ =1, R_d=3

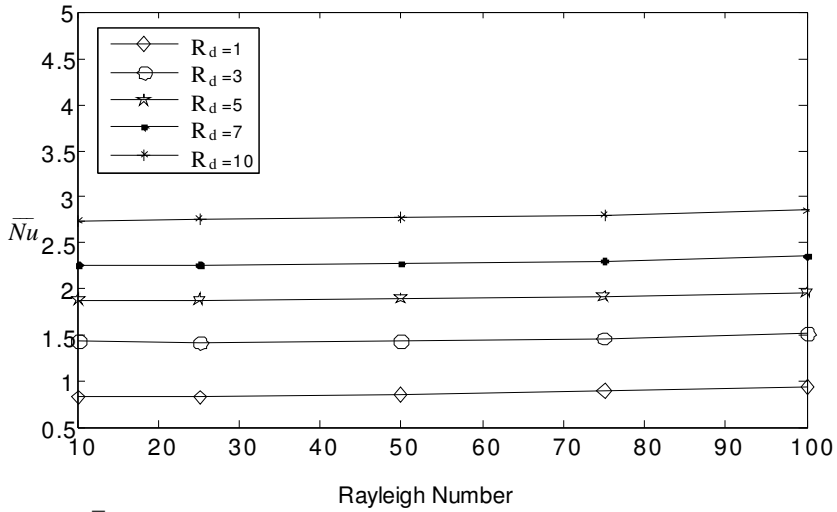

Fig. 12. $\bar{N}u$ Variations with Ra at hot surface for different values of R_d at λ =1, A_r =1.

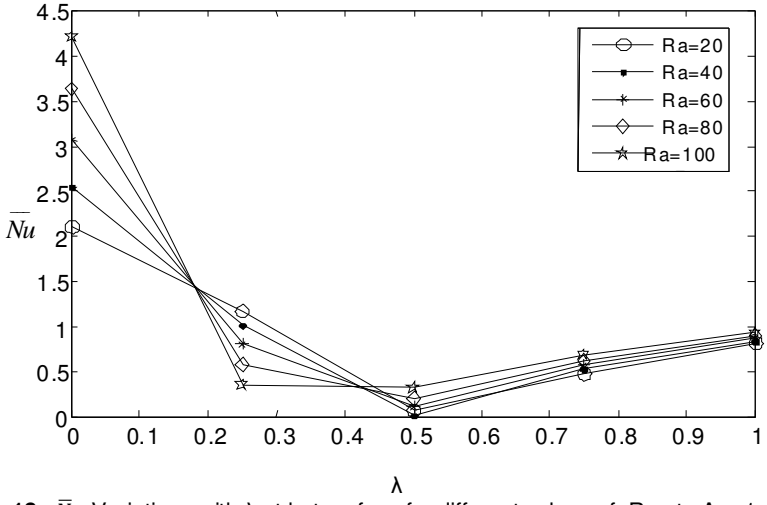

Fig. 13. $\bar{N}u$ Variations with λ at hot surface for different values of Ra at Ar =1, Rd=1.

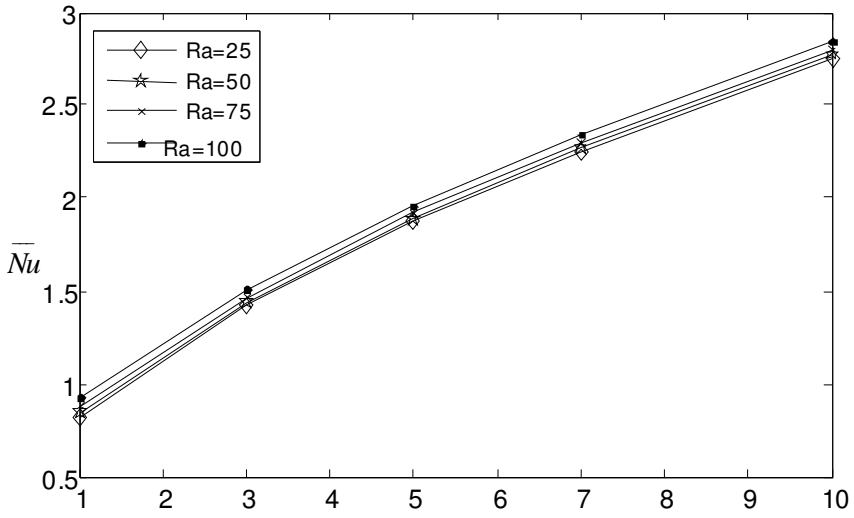

Fig. 14. $\overline{Nu}$ Variations with R_d at hot surface for different values of Ra at A_r =1, λ =1.

Fig. 14 shows the variation of $\overline{Nu}$ with respect to R_d for hot surface at different values of Ra at A_r =1, λ = 1. $\overline{Nu}$ Increases with increase in R_d, the line is corresponds to different Ra come close there is no change even the R_d is maximum.

VI. CONCLUSIONS

- The magnitude of the streamlines decreases when λ as increase from 0 to 1 is and streamlines tend to move towards upper horizontal wall.
- The isotherms thickness of the thermal boundary layer becomes small with increase in λ.
- The increased Raleigh numbers is associated with higher convection heat transfer thus the streamlines crowded and covers almost whole domain.
- The area occupied by the temperature lines decreases when Ra is maximum.
- Increase in A_r the streamlines are distorted and crowded near upper horizontal wall of the cavity, indicating the increasing fluid velocity at that position. Particularly near Ar = 2 we observe convective effect is observed at lower left, upper right corners of the cavity.
- The flow consists of a single cell and it is clear from the streamlines that the velocity of the fluid increases with increase in R_d form isotherms. We conclude that the thermal boundary layer become thin.

REFERENCES

[1]. Ostrach, S., (1972). Natural convection in enclosures. *Advances in Heat Transfer*, Vol. **VIII**, Academic press, New York, pp.161-227.

[2]. Patterson, J. and Limburger, J., (1980). Unsteady natural convection in a rectangular cavity. *Int. J. Fluid Mech.,* Vol. **100**, pp. 65-86.

[3]. Segerland, L. (1982). Applied Finite element analysis. John wiley & Sons, New York.

[4]. Kirkpatrick, T. and Bohn, M., (1986). An experimental investigation of mixed cavity natural convection in the high Rayleigh number regime. *Int. J. Heat Mass Transfer*, Vol. **29**, pp. 69-82.

[5]. November, M. and Nansteel, M.W.(1987). Natural convection in rectangular enclosures from below and cooled along one side. *Int. J. Heat Mass Transfer*, Vol. **30**, pp. 2433-2440.

[6]. Hall, J.D., Bejan, A. and Chaddock, J.B. (1988). Transient natural convection in a rectangular enclosure with one heated side wall. *Int. J. Heat Fluid Flow*, Vol. **9**, pp. 396-404.

[7]. Frederick Valencia, R.L. (1989). Heat transfer in square cavities with partially active vertically walls. *Int. J. Heat Mass Transfer*, Vol. **32**, pp.157-1574.

[8]. Fusegi. T., Hyun, J.M. and Kuwahara, K. (1992). Natural convection in a differentially heated square cavity with internal heat generation. *Num. Heat Transfer Part A*, Vol. **21**, pp. 215-229.

[9]. Ganzarolli, M.M. and Milanez, L.F. (1995). Natural convection in rectangular enclosures heated from below and symmetrically cooled from the sides. *Int. J. Heat Mass Transfer*, Vol. **38**, **pp**.1063-1073.

[10]. Aydin. O, Unal. and Ayhan. T. (1999). Natural convection in rectangular enclosures heated from one side and cooled from the ceiling. *Int. J. Heat Mass Transfer*, Vol. **5**, pp. 2345-2355.

[11]. Kairi. R.R. and Murthy, P.V.S.N. (2009). Free Convection in a Thermally Stratified Non-Darcy Porous Medium Saturated with a Non-Newtonian Fluid. *Int. J. of Fluid Mech. Res*, Vol. **36** (5): 414-423.

[12]. Asterios, P. and Eugun, M. (2010). Forced Convection Flow of Power-Law Fluids Over a Flat Plate Embedded in a Darcy-Brinkman Porous Medium. *Transport in Porous Media*, Vol**. 85**: 143-155.

[13]. Mansour, M.A. and Ahmed. S.E. (2015). A numerical study on natural convection in porous media-filled an inclined triangular enclosure with heat sources using nano-fluid in the presence of heat generation effect. *Engineering Science and Technology, an International Journal*, Volume **18**, Issue 3, pp. 485-495.

[14]. Vargas. M, Tatsios. G., Valougeorgis, D. and Stefanov, S. (2016). Rarefied gas flow in a rectangular enclosure induced by non-isothermal walls. *Physics of Fluids,* **26**(5): 057101-057123.

[15]. Sparrow, E.M., Kruger, P.D. and Heinisch, R.P. (2010). Radiation from Cavities With Non-isothermal Heat Conducting Walls. *J. Heat Transfer,* **96**(1): 15-20.
[16]. Mahapatraa, T.R., Pal, D. and Sabyasachi, M. (2012). Combined effects of thermal radiation and heat generation on natural convection in a square cavity filled with Darcy-Forchheimer porous medium". *Int. Journal of Applied Mathematics and Computation,* vol. **4**, pp.11-18.
[17]. Lamsaadi, M., Naïmi, M., Hasnaoui, M. and Mamou, M. (2003). Natural Convection in a Vertical Rectangular Cavity Filled with a Non-Newtonian Power Law Fluid and Subjected to a Horizontal Temperature Gradient. An *International Journal of Computation and Methodology,* Vol. **49**, Issue 10, pp.969-990.
[18]. Ohta, M., Akiyoshi, M. and Obata, E. (2002). A Numerical Study on Natural Convective Heat Transfer of Pseudoplastic Fluids in a Square Cavity. *An International Journal of Computation and Methodology*, Vol. **41**, Issue 4, pp. 357-372.

How to cite this article: Devi, K.G. and Babu, K.V. (2019). A Convective Heat Flow in a Rectangular Cavity with Effect of Non-Isothermal Wall. *International Journal on Emerging Technologies*, **10**(2): 78-93.